

Hypoxic Tumor-Derived Exosomal miR-301a Mediates M2 Macrophage Polarization via PTEN/PI3K γ to Promote Pancreatic Cancer Metastasis



Xiaofeng Wang¹, Guangtao Luo¹, Kundong Zhang¹, Jun Cao¹, Chen Huang¹, Tao Jiang¹, Bingya Liu², Liping Su², and Zhengjun Qiu¹

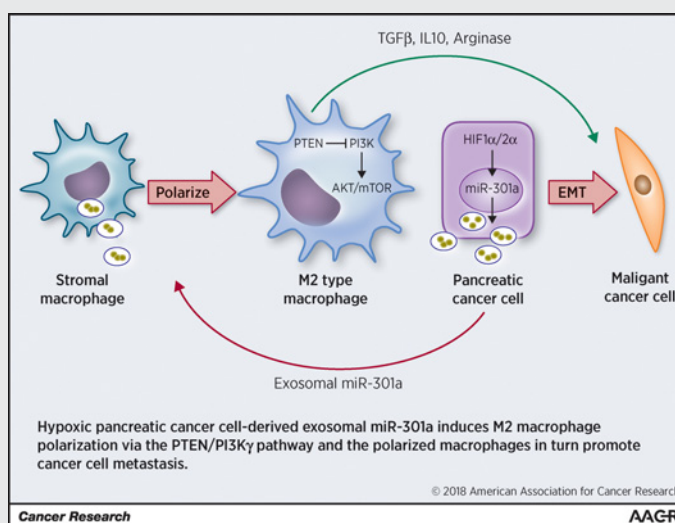
Abstract

Exosomes are emerging as important mediators of the cross-talk between tumor cells and the micro-environment. However, the mechanisms by which exosomes modulate tumor development under hypoxia in pancreatic cancer remain largely unknown. Here, we found that hypoxic exosomes derived from pancreatic cancer cells activate macrophages to the M2 phenotype in a HIF1 α or HIF2 α -dependent manner, which then facilitates the migration, invasion, and epithelial–mesenchymal transition of pancreatic cancer cells. Given that exosomes have been shown to transport miRNAs to alter cellular functions, we discovered that miR-301a-3p was highly expressed in hypoxic pancreatic cancer cells and enriched in hypoxic pancreatic cancer cell-derived exosomes. Circulating exosomal miR-301a-3p levels positively associated with depth of invasion, lymph node metastasis, late TNM stage, and poor prognosis of pancreatic cancer. Hypoxic exosomal miR-301a-3p induced the M2 polarization of macrophages via activation of the PTEN/PI3K γ signaling pathway. Coculturing of pancreatic cancer cells with macrophages in which miR-301a-3p was upregulated or treated with hypoxic exosomes enhanced their metastatic capacity. Collectively, these data indicate that pancreatic cancer cells generate miR-301a-3p-rich exosomes in a hypoxic microenvironment, which then polarize macrophages to promote malignant behaviors of pancreatic cancer cells. Targeting exosomal miR-301a-3p may provide a potential diagnosis and treatment strategy for pancreatic cancer.

Significance: These findings identify an exosomal miRNA critical for microenvironmental cross-talk that may prove to be a potential target for diagnosis and treatment of pancreatic cancer.

Graphical Abstract: <http://cancerres.aacrjournals.org/content/canres/78/16/4586/F1.large.jpg>. *Cancer Res*; 78(16); 4586–98.

©2018 AACR.



Introduction

Pancreatic cancer is one of the most notorious carcinomas and is projected to become the second leading cause of cancer-

¹Department of General Surgery, Shanghai General Hospital, Shanghai Jiao Tong University School of Medicine (originally named "Shanghai First People's Hospital"), Shanghai, P.R. China. ²Department of Surgery, Shanghai Key Laboratory of Gastric Neoplasms, Shanghai Institute of Digestive Surgery, Ruijin Hospital, Shanghai Jiao Tong University School of Medicine, Shanghai, P.R. China.

Note: Supplementary data for this article are available at Cancer Research Online (<http://cancerres.aacrjournals.org/>).

Corrected online February 14, 2020.

X. Wang and G. Luo contributed equally to this article.

related death in the United States (1). Although appropriate surgical resection and adjuvant treatments such as chemotherapy are used to treat pancreatic cancer, an overall 5-year survival rate is still less than 5% and the median survival is only about

Corresponding Authors: Zhengjun Qiu, Shanghai General Hospital, Shanghai Jiao Tong University School of Medicine (originally named "Shanghai First People's Hospital"), Shanghai 200080, China. Phone: 8621-6307-9675; Fax: 86-21-63079675; E-mail: qiuizdoctor@sina.com; and Liping Su, Department of Surgery, Shanghai Key Laboratory of Gastric Neoplasms, Shanghai Institute of Digestive Surgery, Ruijin Hospital, Shanghai Jiao Tong University School of Medicine, Shanghai 200025, P.R. China. E-mail: suliping@shsmu.edu.cn

doi: 10.1158/0008-5472.CAN-17-3841

©2018 American Association for Cancer Research.

3–6 months (2, 3). The high mortality in patients with pancreatic cancer is mainly ascribed to the difficult diagnosis at the early stage, aggressive local invasion, and early metastasis (4, 5). Therefore, the discovery of new diagnostic biomarkers and a better understanding of molecular mechanisms underlying the metastasis of pancreatic cancer are crucial.

Tumor metastasis is closely correlated with tumor microenvironment in which hypoxia and inflammatory cells infiltration especially macrophages are two important factors (6, 7). Hypoxia, defined as a condition where the oxygen pressure is less than 5–10 mm Hg, is a powerful driving force for cancer metastasis processes from the initial epithelial–mesenchymal transition (EMT) to the ultimate organotropic colonization (8). The major mechanism mediating cellular responses to hypoxia is stabilization and activation of hypoxia-inducible factors (HIF), especially HIF1 α and HIF2 α , which activate a set of genes that facilitate tumor growth, angiogenesis, and metastasis (9, 10). Exosomes, produced by many cell types including dendritic cells, B cells, T cells, mast cells, epithelial cells, and tumor cells, are tiny vesicles, 30–150 nm in size, that are formed during endocytosis (11). Typical exosomes contain a wide range of functional mRNAs, miRNAs, and proteins, playing an essential role in intercellular communication through transferring their genetic contents (11, 12). Recent study indicated that hypoxia might promote tumor progression via altering exosomes release to regulate cell–cell communication (13). Exosomes derived from tumor cells contribute to the development of cancer through communication between the tumor and surrounding stromal tissue, activation of proliferative and angiogenic pathways, initiation of premetastatic sites, and formation of immune suppression (12, 14–16). Tumor cells may generate miR-21–rich exosomes that are delivered to normoxic cells to promote prometastatic behaviors under hypoxia (17).

Macrophages, the most abundant infiltrative immune-related stromal cells present in and around tumors, display diverse phenotypes and functions (18). Macrophages can be polarized into classically (M1) or alternatively (M2) activated cells depending on environmental cues. M1 macrophages characterized by the expression of the inducible type of nitric oxide synthase (iNOS) are proinflammatory, whereas M2 macrophages express high level of anti-inflammatory cytokines (e.g., IL10) and a potent arginase-1 (Arg1) activity to favor tumor cell growth (19–21). However, the mechanisms underlying macrophages polarization remain largely unknown in pancreatic cancer. In this study, we demonstrate that pancreatic cancer cell–derived exosomes express miR-301a-3p in hypoxia microenvironment, and can polarize macrophages via PTEN/PI3K γ signaling pathway. The polarization of M2 macrophages lead to the enhanced metastatic potential of pancreatic cancer cells *in vitro* and *in vivo*. Thus, the data implicate miR-301a-3p as a target for exosome-mediated tumor immune evasion.

Materials and Methods

Patient samples and ethical statement

Pancreatic cancer blood samples were collected from 50 patients between 2013 and 2015 at the Ruijin Hospital and Shanghai General Hospital, Shanghai, China and healthy blood samples were obtained from 12 volunteers without any malignancy. The study was approved by the Ethics Committee of Shanghai General Hospital and Ruijin Hospital, Shanghai Jiao-

tong University School of Medicine, and conducted in accordance with ethical principles of the World Medical Association Declaration of Helsinki and local legislation. Informed consent was written by all patients prior to this study.

Cell culture and hypoxia treatment

Pancreatic cancer cell lines PANC-1, BxPC-3, and monocytic cell line THP-1 were obtained from the ATCC. They have been authenticated by a STRDNA profiling analysis and routinely examined for *Mycoplasma* contamination. Human bone marrow–derived macrophages (HBMDM) were isolated and induced from human bone marrow. The cell lines were maintained at 37°C in a humidified atmosphere of 5% CO₂ with RPMI1640 medium containing 10% fetal bovine serum (FBS) with 100 U/mL penicillin G and 100 μ g/mL streptomycin sulfate. To induce differentiation into macrophages, THP-1 cells (1×10^6) were incubated with 100 ng/mL PMA (Sigma) for 24–48 hours. For exosome isolation, PANC-1 and BxPC-3 cells were cultured in a hypoxia cell incubator of 1% O₂ with contained exosome-depleted FBS (SBI) medium.

Exosome isolation and identification

The cell lines were cultured in the normal medium until 80%–90% confluent; thereafter, medium was replaced with RPMI1640 with 10% exosome-depleted FBS and cultured under normoxic or hypoxic (1% O₂) conditions. Then, the cell culture medium was harvested after 3 days (30 mL) and centrifuged at 300 \times g for 10 minutes, 2,000 \times g for 10 minutes, 10,000 \times g for 30 minutes to remove residual cells and debris, and ultracentrifuged at 100,000 \times g for 70 minutes (Beckman Coulter) to collect the pellet that was resuspended in 50–100 μ L PBS (22). The exosomes were also isolated by a precipitation method using Exoquick Reagent (SBI) according to the manufacturer's instruction. Briefly, conditioned media were incubated with Exoquick reagent (5:1) for over 12 hours, centrifuged at 1,500 \times g for 30 minutes and pelleted exosomes were resuspended in 100- μ L PBS and stored at –80°C until further use. In addition, the isolation of serum exosomes was used by total exosomes isolation reagent (Magen). The reagent was added to the serum samples and incubated at 4°C for 30 minutes prior to serum samples (1 mL) being centrifuged at 2,000 \times g for 30 minutes to remove cells and debris. Exosomes were obtained by centrifugation at 10,000 \times g for 10 minutes and resuspended in 200- μ L PBS.

The size of exosomes was analyzed using Nanosight LM10 System (Nanosight Ltd) equipped with a fast video capture and particle-tracking software via measuring the rate of Brownian motion to calculate nanoparticle concentrations and size distribution. Besides, exosomes to be examined by transmission electron microscopy were suspended in glutaraldehyde, dropped in carbon-coated copper grids, stained with 2% uranylacetate, dried, and imaged.

Exosome labeling and tracking

Purified exosomes isolated from the culture medium were collected and labeled with PKH67 Green Fluorescent membrane linker dye (Sigma-Aldrich) according to manufacturer's instructions. Then, the labeled exosome pellets were resuspended and added to the unstained macrophages for exosomes uptake studies. After incubation for 30 minutes, 2 hours, or 12 hours at 37°C, cells were observed by fluorescence microscopy.

Luciferase assays

The 293T cells were cotransfected with wild-type or mutant PTEN 3'-UTR psiCHECK-2 plasmid (Promega) and miR-301a-3p/mimics or control and miR-301a-3p/inhibitor (Ribo) using Lipofectamine 3000 (Invitrogen). Cell lysates were harvested 48 hours after transfection and then firefly and *Renilla* luciferase activities were measured by a dual luciferase reporter assay kit according to the manufacturer's protocol. *Renilla* luciferase activity was used for normalization.

Quantitative real-time PCR

Total RNA from cells and exosomes was extracted using TRIzol reagent (Invitrogen) and complementary DNA was synthesized with Reverse Transcription system (Toyobo) according to the manufacturer's instructions. Real-time PCR was performed using SYBR Green PCR Master Mix (Applied Biosystems). Expression data were uniformly normalized to the internal control U6 and the relative expression levels were evaluated using the $\Delta\Delta C_t$ method. In addition, cel-miR-39 was used to normalize for technical variation between exosomes samples as described previously (23). The primers of miR-301a-3p, cel-miR-39, and U6 were purchased from Ribo. The primer sequences used were as follows: CD206 primers, forward: 5'-GGGTTGCTATCACTCTC-TATGC-3', reverse: 5'-TTTCTGTCTGTGCGGTAGTT-3'; Arg-1 primers, forward: 5'-GGTTTTGTGTGCGGTGTTT-3', reverse: 5'-CTGGGATACTGATGGTGGGATGT-3'; CD163 primers, forward: 5'-TTTGCAACTTGAGTCCCTTCAC-3', reverse: 5'-TCCC-GCTACACTGTTTTTAC-3'; CD68 primers, forward: 5'-CTTCT-CTCATTCCCCTATGGACA-3', reverse: 5'-GAAGGACACATTGTA-CTCCACC-3'; TGF β primers, forward: 5'-CAATTCCTGGCGA-TACCTCAG-3', reverse: 5'-GCACAACCTCCGGTGACATCAA-3'; IL10 primers, forward: 5'-GACTTTAAGGGTACCTGGGTG-3', reverse: 5'-TCACATGCGCCTTGATGTCTG-3'; IL1 β primers, forward: 5'-ATGATGGCTTATTACAGTGGCAA-3', reverse: 5'-GTCC-GAGATTTCGTAGCTGGA-3'; iNOS primers, forward: 5'-AGGGA-CAAGCCTACCCCTC-3', reverse: 5'-CTCATCTCCCCTCAGTTGG-T-3'; PTEN primers, forward: 5'-TGGATTCGACTTAGACTTGAC-CT-3', reverse: 5'-GGTGGGTATGGTCTTCAAAGG-3'; HIF1 α primers, forward: 5'-GAACGTGCAAAAAGAAAAGTCTCG-3', reverse: 5'-CCTTATCAAGATGCGAACTCACA-3'; HIF2 α primers, forward: 5'-CGGAGGTGTTCTATGAGCTGG-3', reverse: 5'-AGCTTGTGTGTTCCGAGGAA-3'.

Western blot analysis

Cells or exosomes were lysed in RIPA lysis buffer with complete protease and phosphatase inhibitor cocktails (Sigma). A total of 30 μ g of protein per sample was loaded onto SDS-PAGE gels and then transferred onto 0.22- μ m polyvinylidene difluoride membranes (Millipore). Membranes were blocked and incubated with primary antibodies at 4°C for overnight, following by incubation with the horseradish peroxidase-conjugated secondary antibody at room temperature. Finally, the membranes were visualized with Thermo Pierce chemiluminescent (ECL) Western Blotting Substrate (Thermo Fisher Scientific) using a Tanon 5200 system (Tanon). The primary antibodies used in the experiments were anti-CD9, anti-CD81, anti-TSG101, anti-HSP70, anti-ALIX, anti-CD206, anti-arginase-1, anti-Flotillin-1 (1:500; Santa Cruz Biotechnology); anti-E-cadherin, anti-N-cadherin, anti-vimentin, anti-MMP7 (1:1,000; Proteintech); anti-mTOR, anti-p-mTOR, anti-AKT, anti-p-AKT (1:1,000; Cell Signaling Technology), and anti-GAPDH (1:10,000).

RNA interference

The PI3K γ siRNA (Extended Nature Biotech) and miR-301a-3p/mimics or inhibitors (GenePharma) at a final concentration of 100 nmol/L were transfected into macrophages with Lipofectamine 2000 reagent (Invitrogen) according to the manufacturer's instructions. The PI3K γ siRNA#1 sense was 5'-GCUUUUAGUU-CAGUGAAAdTdT-3' and antisense was 5'-UUUCACUGAA-CUAAAUAGCdTdT-3'. The PI3K γ siRNA#2 sense was 5'-GGAC-GAUGAUGUUCUGCAUdTdT-3' and antisense was 5'-AUGCA-GAACAUCAUCGUCCdTdT-3'. Cells were collected for further assay at 24, 48, and 72 hours after transfection. The miR-301a sgRNA-targeting sequences were TGATACCGAAGAAAGATGTA. The miR-301a sgRNA primers were miR-301a-3p-3'-cas9-Forward: CACCGTGATACCGAAGAAAGATGTA and miR-301a-3p-3'-cas9-Reverse: AACTACATCTTCTTCGGTATCAC.

Cell migration and invasion

Cell migration and invasion assays were performed using 24-well plates and 8- μ m transwell inserts (Corning Life Science). For migration assays, tumor cells (5×10^4) suspended in 200 μ L serum-free medium were seeded into the top chamber, and 1×10^4 macrophages in 800 μ L medium containing 10% FBS were added to the bottom chamber. For the invasion assay, the insert membranes were coated with Matrigel (50 μ L/well; BD Biosciences) before adding the cells. After 24 hours of culture, cells were then stained with 0.1% crystal violet for 30 minutes, and nonmigrating or noninvading cells were removed. Six visual fields were randomly chosen to calculate the number of migrated cells.

IHC

IHC staining was conducted using streptavidin-biotin-peroxidase complex method. Briefly, pancreatic cancer tissue samples were fixed, paraffin-embedded, dewaxed, rehydrated, and antigen retrieval. Then samples were stained with CD9 or CD163 antibody at 4°C overnight, followed by incubation in secondary biotinylated antibody for 30 minutes at 37°C, and finally visualized with DAB solution and counterstained with hematoxylin. Pictures were taken under a light microscope.

In vivo metastasis

Male BALB/c nude mice (4-week-old; Institute of Zoology, Chinese Academy of Sciences, Beijing, China) were housed at a specific pathogen-free environment in the Animal Laboratory Unit of Ruijin Hospital, Shanghai Jiaotong University School of Medicine (Shanghai, China). All animal experiments were approved by the Institutional Animal Care and Use Committee and performed according to the institution's guidelines and animal research principles. Twenty-five mice were randomly divided into five groups (5 mice per group). PANC-1 cells mixed with the conditioned macrophages stimulated by hypoxic PANC-1-exo or transfected by miR-301a-3p/mimics were injected into the mice via tail vein to observe the distant metastasis. After 6 weeks, all mice were sacrificed under general anesthesia after injection. All the suspicious lung metastasis sites were evaluated by histologic examination.

Statistical analysis

The experimental results were repeated at least three times and were shown as mean \pm SEM (parametric data) or median \pm range (nonparametric data). The association between exosomal

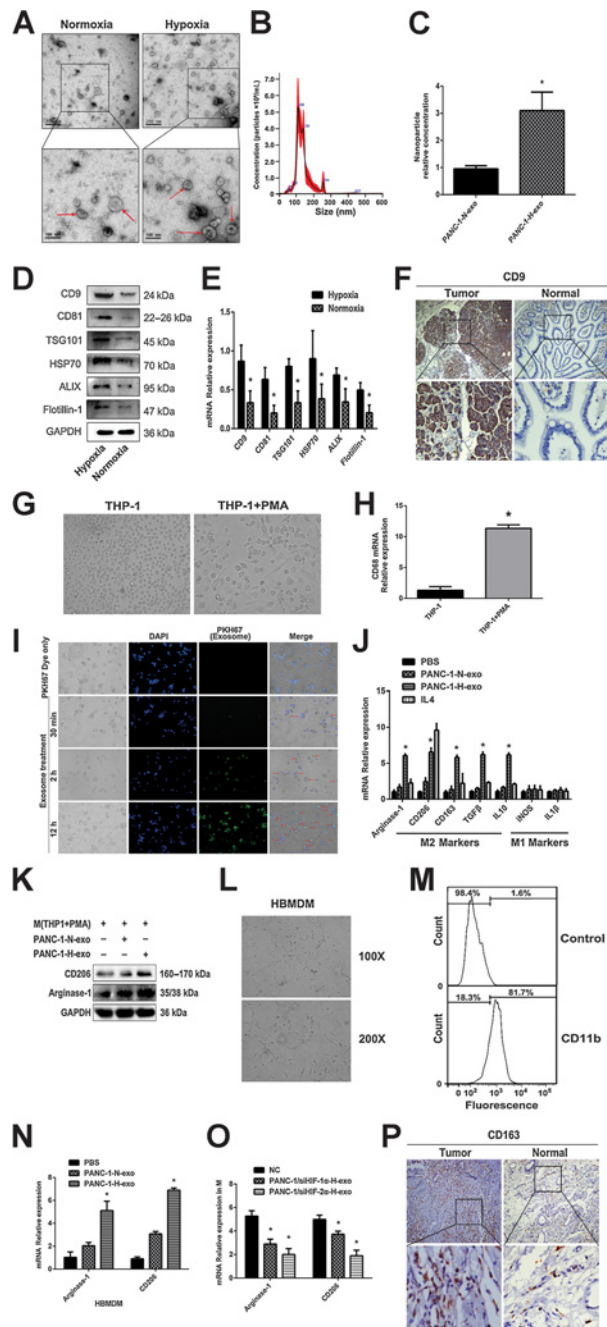


Figure 1. Hypoxia promotes exosome secretion from pancreatic cancer cells that induce the polarization of M2 macrophages. **A**, Electron microscopy images of exosomes isolated from conditioned medium of PANC-1 cells under normoxia and hypoxia (PANC-1-H-exo). **B**, NTA of PANC-1-H-exo isolated by ultracentrifugation. **C** and **D**, Identical concentrations of PANC-1 cells were seeded under normoxia and hypoxia. Exosomes (PANC-1-N-exo and PANC-1-H-exo) were purified for NTA and Western blot analysis. PANC-1-exo nanoparticle relative concentration (**C**); Western blot analysis for exosomal proteins CD9, CD81, TSG101, HSP70, ALIX, and Flotillin-1 (**D**). GAPDH in cell extracts was used as control for cell density. **E**, Protein ratio of CD9, CD81, TSG101, HSP70, ALIX, and Flotillin-1 in exosomes (*, $P < 0.05$). **F**, Expression of CD9 was examined by IHC in pancreatic cancer tissues. **G**, THP-1 cells were treated with phorbol-12-myristate-13-acetate (PMA) for 24 hours.

miR-301a-3p expression and clinicopathologic characteristics was statistically determined using the Pearson χ^2 test. Differences between treated and control groups were analyzed using the Student *t* test or one-way ANOVA. Survival curves were estimated using the Kaplan–Meier method, and the log-rank test was used to calculate differences between the curves. A two-tailed value of $P < 0.05$ was considered statistically significant. All statistical analyses were performed with the SPSS 13.0 statistical software (SPSS Inc.).

Results

Hypoxia promotes exosomes secretion of pancreatic cancer cells to induce macrophages M2 polarization

To examine the impact of hypoxia on exosomes released from pancreatic cancer cells, identical concentrations of PANC-1 cells were seeded under normoxia and hypoxia (1% O_2). Exosomes were isolated from the conditioned media after 48 hours and quantitated by electron microscopy and nanoparticle tracking analysis (NTA). As shown in Fig. 1A and B, electron microscopy revealed typical rounded particles ranging from 30 to 150 nm in diameter, and NTA exhibited a similar size distribution of exosomes. Moreover, exosomes harvested from hypoxic PANC-1 cells demonstrated significantly higher nanoparticle concentrations compared with that from the normoxic control (2.89-fold; $P < 0.05$; Fig. 1C). Western blot analysis of proteins extract from exosomes confirmed the presence of the exosomal proteins CD9, CD81, TSG101, HSP70, ALIX, and Flotillin-1 (Fig. 1D), as identified in the ExoCarta database (24), and increased levels of CD9, CD81, TSG101, HSP70, ALIX, and Flotillin-1 levels were observed in PANC-1 exosomes after exposure to 1% O_2 for 48 hours (Fig. 1D and E). Consistent with these observations, expression level of CD9 (exosomes marker) examined by IHC in pancreatic cancer tissues was significantly higher than nontumor pancreatic tissues (Fig. 1F). Thus, these results demonstrated that hypoxia enhances pancreatic cancer cells' exosomes secretion.

Hypoxia is one of the important features in solid tumors and exosomes, once secreted, could deliver biologic information by internalization to neighboring or distant cells (8, 11). Macrophages are the most abundant infiltrative immune-related stromal cells present in and around tumors, we then investigated whether hypoxic tumor cell-derived exosomes could affect the

Representative image of macrophages is shown. **H**, qRT-PCR was used to detect the expression of CD68 (macrophage marker). **I**, Representative immunofluorescence image shows the internalization of PKH67-labeled PANC-1-derived exosomes (green) by macrophages. **J**, Macrophages were treated with PANC-1-N-exo, PANC-1-H-exo (100 $\mu\text{g}/\text{mL}$), or control (PBS and IL4). After 48 hours, qRT-PCR was applied using primers for M2 markers (CD206, CD163, TGF β , IL10, arginase-1) and M1 markers (iNOS, IL1 β). The group treated with IL4 was used as positive control. **K**, Western blot analysis was used to detect M2 marker CD206 and arginase-1. **L**, The morphology of HBMDM. **M**, Flow cytometry was used to detect the expression of macrophages marker (CD11b) in HBMDM. **N**, qRT-PCR was used to examine the M2 markers (CD206, CD163) expression of HBMDM treated with PANC-1-N-exo, PANC-1-H-exo (100 $\mu\text{g}/\text{mL}$), or PBS. **O**, qRT-PCR was used to detect the expression of CD206 and arginase-1 in the macrophages treated with hypoxic exosomes from PANC-1 transfected with HIF1 α siRNA or HIF2 α siRNA. **P**, Expression of CD163 was examined by IHC in pancreatic cancer tissues. Data are shown as mean \pm SD of three independent experiments (*, $P < 0.05$).

polarization of macrophages. As shown in Fig. 1G and H, human THP-1 monocytes were differentiated into macrophages by an incubation in the presence of phorbol 12-myristate 13-acetate (PMA), which is characterized by the adherent morphology and the expression of recognized macrophage marker CD68. We next examined the effects of hypoxic exosomes on macrophages' polarization. As shown in Fig. 1I, when cocultured with macrophages, tumor-derived hypoxic exosomes labeled with fluorescent PKH67 were internalized by unstained macrophages over time. The expression of M2 markers (CD206, CD163, IL10, TGF β , and arginase-1) increased in macrophages incubated with hypoxic exosomes compared with normoxic exosomes or PBS (Fig. 1J and K). Consistent with the observation above, the M2 markers (CD206, CD163) expression of HBMDM (Fig. 1L and M) treated with PANC-1-H-exo also increased (Fig. 1N). However, the effect of exosomes on the M2 polarization of macrophages was impaired when downregulating the expression of HIF1 α or HIF2 α in PANC-1 cells under hypoxia, which were demonstrated by less expression of CD206 and arginase-1 (Fig. 1O; Supplementary Fig. S1A and S1B). In addition, CD163 is associated with the activation of macrophage toward M2 phenotype, and higher densities of cells expressing M2 macrophage-associated marker CD163 were found in pancreatic cancer tissues compared with matched nontumor pancreatic tissue (Fig. 1P). Thus, these results demonstrated that hypoxia enhances pancreatic cancer cells exosomes secretion to activate macrophage toward M2 phenotype via HIF-1 α and HIF-2 α .

M2 macrophages induced by hypoxic exosomes promote the migration, invasion, and EMT of pancreatic cancer cells

We next studied the role of M2 macrophages induced by hypoxic pancreatic cancer cell-derived exosomes in the migration, invasion, and EMT of pancreatic cancer cells using the *in vitro* indirect coculture system (Fig. 2A). Migration and invasion transwell assays showed that M2 macrophages (M: THP-1 with PMA, BMDM: bone marrow-derived macrophages) induced by hypoxic tumor-derived exosomes significantly increased the migration and invasion of pancreatic cancer cells (BxPC-3 and PANC-1) compared with normoxic exosomes (Fig. 2B–G). In addition, we further assessed whether activated M2 macrophages regulate EMT of pancreatic cancer cells. As shown in Fig. 2H, after coculturing with M2 macrophages induced by hypoxic tumor-derived exosomes for 24 hours, BxPC-3 cells lost intercellular junctions, extended cellular pseudopod, and acquired a spindle-shaped morphology. Moreover, the expression levels of epithelial cell marker (E-cadherin) decreased and the expression levels of mesenchymal cell markers (N-cadherin, vimentin, and MMP7) increased (Fig. 2I and J). Coincidentally, the same results were obtained in the experiments of PANC-1 cells (Fig. 2K–M). Taken together, these data suggest that activated M2 macrophages induced by hypoxic exosomes promote pancreatic cancer cell migration, invasion, and EMT.

miR-301a is highly expressed in exosomes derived from hypoxic pancreatic cancer cells and can be transferred to human macrophages through the exosomes

It has been reported that exosomes contain a variety of biologically active molecules including miRNAs, and that exosomal miRNA profiles resemble those of the parent cells (25). We previously found that miR-301a-3p was highly expressed in pancreatic cancer cells under hypoxia. To elucidate whether

miR-301a-3p was also highly expressed in exosomes derived from pancreatic cancer cells (BxPC-3 and PANC-1) under hypoxia, we detected the expression of miR-301a-3p by RT-PCR or qRT-PCR. The results indicated the expression of miR-301a-3p in hypoxic pancreatic cancer cell-derived exosomes was markedly upregulated compared with normoxic exosomes (Fig. 3A and B). To study whether hypoxia-induced miR-301a-3p expression depends on HIF-1 α or HIF-2 α , we knocked down the expression of HIF-1 α or HIF-2 α in BxPC-3 and PANC-1 cells by siRNA. In normoxic conditions, cellular and exosomal miR-301a-3p expression levels were apparently low and not significantly affected by either HIF-1 α or HIF-2 α knockdown. In hypoxic conditions, however, both cellular and exosomal miR-301a-3p expression levels were markedly high and knockdown HIF-1 α or HIF-2 α expression significantly decreased both cellular and exosomal miR-301a-3p expression (Fig. 3C and D). These results suggest that both cellular and exosomal miR-301a-3p expression under hypoxia was dependent on both HIF-1 α and HIF-2 α . Consistent with these results, the expression of exosomal miR-301a-3p isolated from serum of patients with pancreatic cancer was significantly higher than that in the healthy individuals group (Fig. 3E). Statistical analysis showed that elevated circulating exosomal miR-301a-3p expression was significantly associated with depth of tumor invasion ($P = 0.009$), lymph node metastasis ($P = 0.021$), and late TNM stage ($P = 0.038$), but not with other clinicopathologic parameters including age, sex etc. (Table 1). Moreover, Kaplan–Meier survival analysis indicated that the survival rate of patients with miR-301a-3p-high expression was significantly lower than those with low expression ($P = 0.0182$, Fig. 3F). By multivariate analysis, miR-301a was a significant and independent prognostic indicator for patients with pancreatic cancer besides age, gender, perineural invasion, and TNM. The Cox regression model showed that higher miR-301a expression was associated with poor overall survival ($P = 0.024$, Fig. 3G).

Exosome-contained bioactive molecules including mRNAs and miRNAs can be delivered to other cells and affect cellular functions (12, 17). Then we detected whether hypoxic tumor-derived exosomes can deliver miR-301a-3p to macrophages. As shown in Fig. 3H, macrophages incubated with hypoxic exosomes expressed higher miR-301a-3p than that with normoxic exosomes or PBS. However, when depleting exosomes by ultracentrifugation, macrophages cultured with the supernatant of pancreatic cancer cells (BxPC-3 and PANC-1) exhibited reduced level of miR-301a-3p compared with those cultured in the normal supernatant (Fig. 3I). Furthermore, miR-301a-3p level was significantly increased in macrophages transfected with the total RNA content extracted from pancreatic cancer cells (BxPC-3 and PANC-1)-secreted exosomes (Fig. 3J). Thus, miR-301a-3p is highly expressed in hypoxic pancreatic cancer cell-derived exosomes, the expression level of which in serum is closely related with prognosis of patients with pancreatic cancer, and can be transferred to human macrophages through the exosomes.

Exosomal miR-301a-3p induces the polarization of M2 macrophages to promote the migration, invasion, and EMT of pancreatic cancer cells

We next determined the role of hypoxic exosome-derived miR-301a-3p in the polarization of M2 phenotype macrophages. miR-301a-3p expression in PANC-1 cells was knocked out with

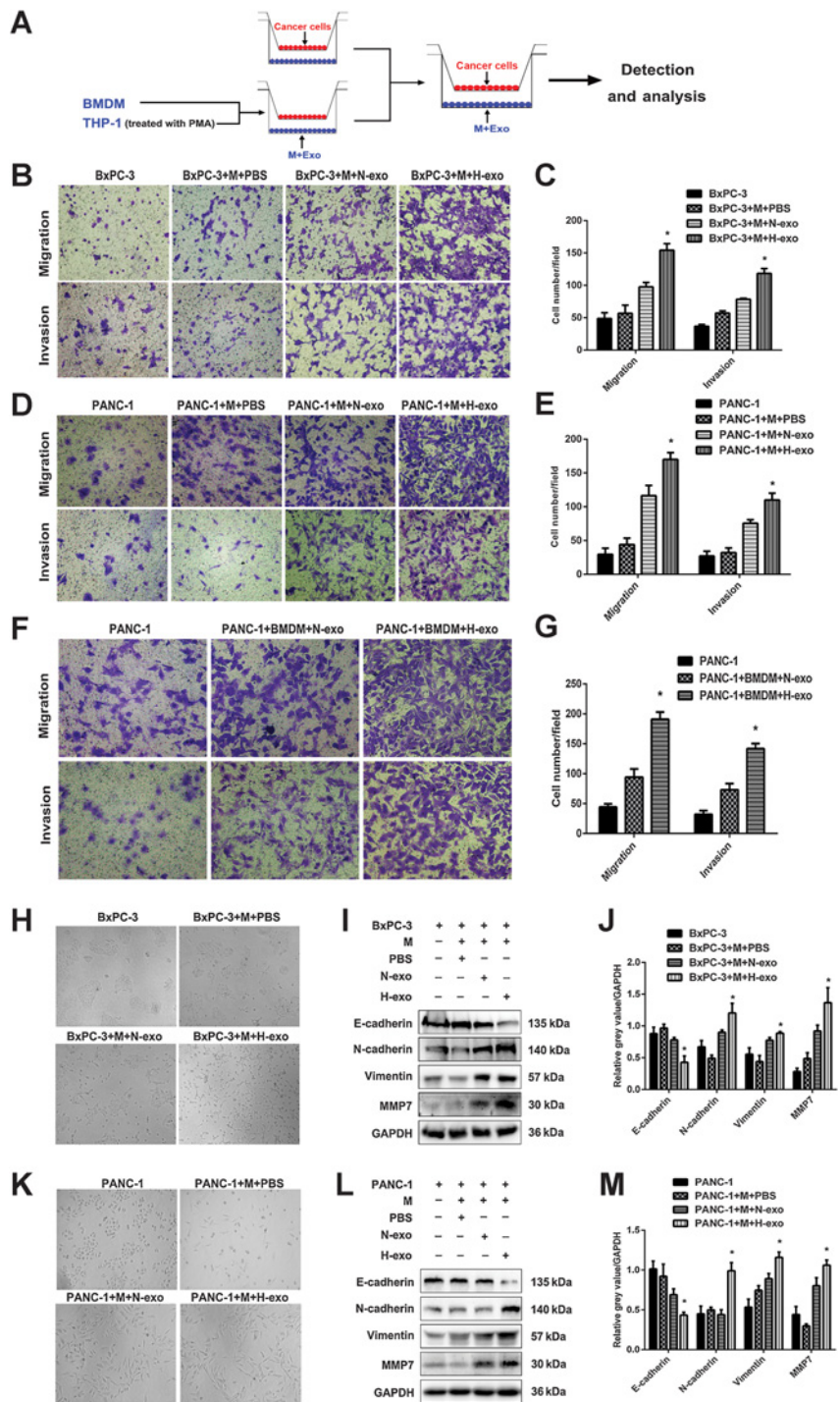


Figure 2.

M2 macrophages polarized by hypoxic exosomes promote the migration, invasion, and EMT of pancreatic cancer cells. **A**, Schematic illustration of the *in vitro* indirect coculture system. **B, D, and F**, Migration and invasion capacity of pancreatic cancer cells (BxPC-3 and PANC-1) cocultured with macrophages (M, THP-1 with PMA; BMDM, bone marrow-derived macrophages) treated with exosomes was determined by the *in vitro* transwell coculture system. Representative photographs of migratory or invaded cells on the membrane coated with or without Matrigel (magnification, $\times 100$) are shown. **C, E, and G**, Morphometric analysis of migratory and invaded cells. **H and K**, The morphology of pancreatic cancer cells (BxPC-3 and PANC-1) incubated with the supernatants of macrophages treated with hypoxic exosomes or control (PBS and normoxic exosomes). **I, J, L, and M**, The effect of the supernatants of macrophages treated with hypoxic exosomes on the EMT of pancreatic cancer cells (BxPC-3 and PANC-1) was analyzed by Western blot analysis. Densitometry shows relative protein expression normalized for GAPDH. Data are representative of three independent experiments (* , $P < 0.05$).

CRISPR/Cas9, then the size distribution and concentration of exosomes derived from PANC-1 cells transfected with miR-301a-3p sgRNA were analyzed by the Nanosight LM10. As shown in Fig. 4A and B, although the size distribution of hypoxic exosomes did not change, the concentration of hypoxic exosomes in miR-301a-3p-knockout PANC-1 cells dramatically reduced, which may attribute to miR-301a overexpression enhancing HIF-1 α accumulation (Supplementary Fig. S1C).

Consistent with the result above, decreased CD9, CD81, TSG101, HSP70, ALIX, and Flotillin-1 were observed in hypoxic exosomes derived from miR-301a-3p-knockout PANC-1 cells (Fig. 4C).

We then measured the expression of miR-301a-3p in hypoxic exosomes derived from miR-301a-3p-knockout PANC-1 cells. qRT-PCR showed that the expression of miR-301a-3p in hypoxia PANC-1 cells and exosomes derived from miR-301a-3p-knockout PANC-1 cells was markedly

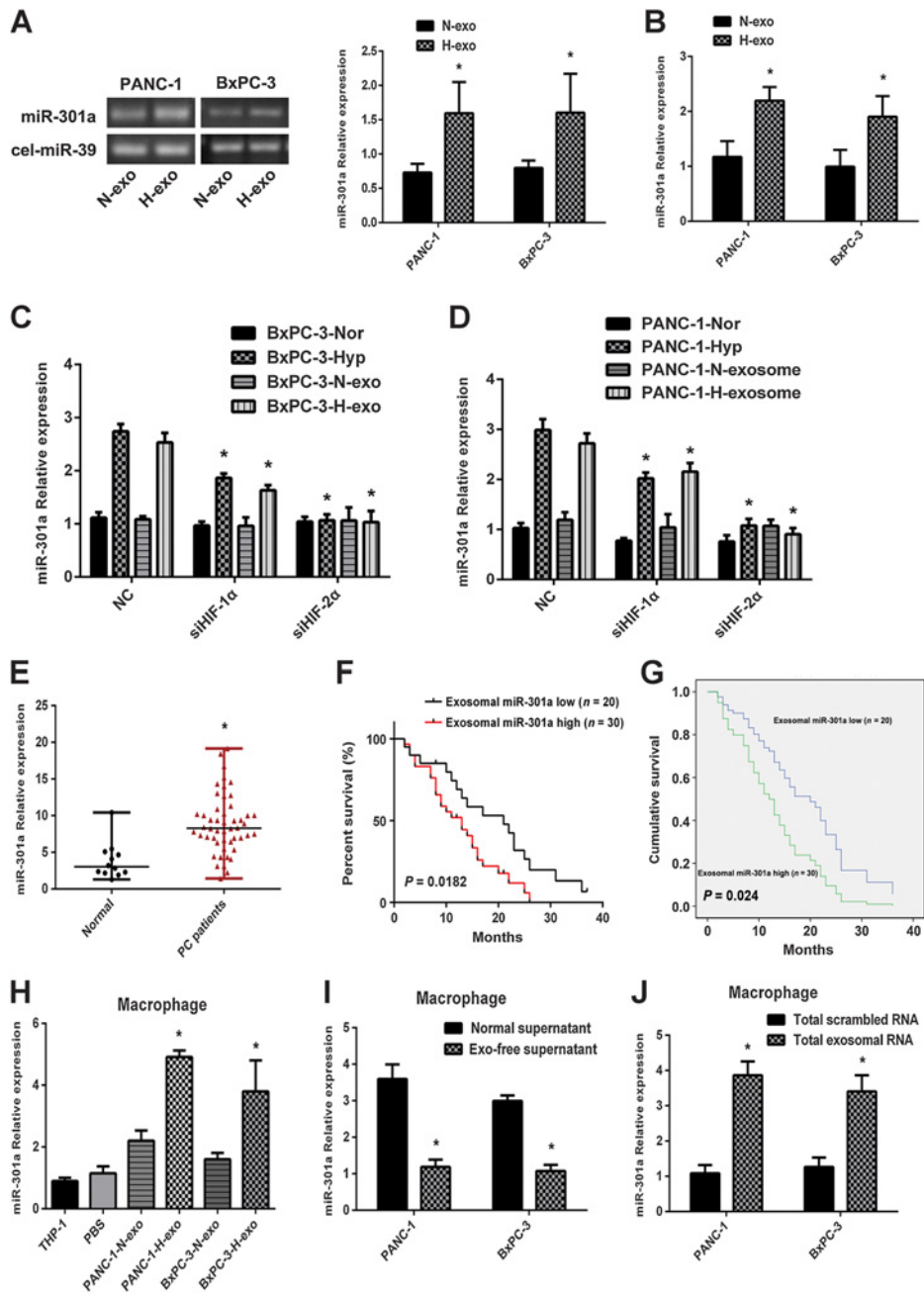


Figure 3. miR-301a is highly expressed in exosomes derived from hypoxic pancreatic cancer cell and serum and can be transferred to human macrophages through the exosomes. **A** and **B**, The miR-301a-3p level was analyzed by RT-PCR or qRT-PCR in pancreatic cancer cell (Bxpc-3 and PANC-1)-derived exosomes under normoxia and hypoxia. **C** and **D**, After transfection with HIF1 α siRNA or HIF2 α siRNA in PANC-1 (or Bxpc-3) cells, miR-301a-3p expression in exosomes and corresponding cells cultured under normoxia or hypoxia was measured by qRT-PCR. **E**, Expression of miR-301a-3p abstracted in serum-derived exosomes from 50 patients with pancreatic ductal adenocarcinoma and 12 healthy individuals was quantified by qRT-PCR. Data are shown as median \pm range (*, $P < 0.05$). **F**, Kaplan-Meier survival curves in human pancreatic cancer according to circulating exosomal miR-301a-3p expression. **G**, Cox regression model after adjusting for age, gender, perineural invasion, and TNM. miR-301a might be an independent predictor of survival, without consideration of age, gender, perineural invasion, or TNM. **H**, Macrophages treated with PBS or pancreatic cancer cell (Bxpc-3 and PANC-1)-derived exosomes for 48 hours; miR-301a-3p expression levels in macrophages were performed by qRT-PCR. **I**, Macrophages cultured with the supernatant of pancreatic cancer cells (Bxpc-3 and PANC-1; normal supernatant) or with exosome depleted by ultracentrifugation (exo-free supernatant) of pancreatic cancer cells for 48 hours; miR-301a-3p expression levels in macrophages were examined by qRT-PCR. **J**, Macrophages transfected with total RNA extracted from exosomes of pancreatic cancer cells (Bxpc-3 and PANC-1; compared with a total scrambled RNA) for 48 hours; miR-301a-3p expression levels in macrophages were detected by qRT-PCR. Relative expression levels of miR-301a-3p in exosomes or macrophages were normalized to cel-miR-39 or U6 snRNA, respectively. Data are presented as mean \pm SD of experiments conducted in triplicate (*, $P < 0.05$).

Downloaded from <http://aacrjournals.org/cancerres/article-pdf/78/16/4586/2771865/4586.pdf> by guest on 27 August 2022

Table 1. Relationship between miR-301a expression and clinicopathologic parameters of 50 patients with pancreatic cancer

Variables	Total	miR-301a expression		P value
		Low (n = 20)	High (n = 30)	
Gender				
Male	29	13	16	0.560
Female	21	7	14	
Age (years)				
≤60	26	9	17	0.106
>60	24	11	13	
T stage				
T1+T2	23	14	9	0.009 ^a
T3+T4	27	6	21	
Lymph node metastasis				
Negative	27	15	12	0.021 ^a
Positive	23	5	18	
TNM stage				
I + II	20	12	8	0.038 ^a
III + IV	30	8	22	
Perineural invasion				
No	28	12	16	0.773
Yes	22	8	14	

^aSignificant difference ($P < 0.05$).

downregulated (Fig. 4D). Moreover, the expression of M2 markers (arginase-1 and CD206) in macrophages cultured with hypoxia exosomes derived from miR-301a-3p-knockout PANC-1 cells also strikingly decreased (Fig. 4E). In addition, the expression of arginase-1 and CD206 in macrophages transfected with the miR-301a-3p mimics was dramatically upregulated (Fig. 4F). Consistent with these observations, both the migration and invasion abilities of BxPC-3 and PANC-1 cells were significantly increased by macrophages transfected miR-301a-3p mimics (Fig. 4G, H, I and J). Furthermore, we examined whether macrophages overexpressing miR-301a-3p induced EMT in pancreatic cancer cells and found that macrophages overexpressing miR-301a-3p markedly enhanced N-cadherin, vimentin, and MMP7 expression while significantly decreasing E-cadherin level in pancreatic cancer cells (Fig. 4K–M). Therefore, hypoxic exosomal miR-301a-3p mediates hypoxic exosome-induced macrophage polarization, which then enhances the migration, invasion, and EMT of pancreatic cancer cells.

Exosomal miR-301a-3p polarized the M2 macrophage via downregulating PTEN expression and activating PI3Kγ signaling pathway

To deeply explore the mechanisms of exosomal miR-301a-3p in the induction of macrophage polarization, we predicted its candidate target gene PTEN by informatics tools (microRNA.org-Targets and Expression software), and then performed luciferase reporter gene assays (Fig. 5A). Luc-PTEN-3'UTR (wild-type, wt) cotransfected with miR-301a-3p/mimics in HEK 293T cells showed a significant decrease of luciferase activity and had a minimal effect on the Luc-PTEN-mut group (Fig. 5B). Conversely, miR-301a-3p/inhibitors increased the luciferase activity of Luc-PTEN-wt compared with Luc-PTEN-mut groups (Fig. 5C). Moreover, overexpression of miR-301a-3p significantly inhibited PTEN mRNA and protein levels in macrophages, while inhibition of miR-301a-3p revealed the opposite effects (Fig. 5D and E). Activation of the PI3Kγ signaling pathway participates in M2 polarization, which facilitates tumor progression (26, 27). Thus, we speculated

hypoxic tumor-derived exosomes could promote polarization of macrophages through PI3Kγ signaling pathway. And the expression of PI3Kγ in macrophages treated with hypoxic exosomes derived from pancreatic cancer cells (BxPC-3 and PANC-1; 100 μg/mL) were determined and the expression level was higher than that in macrophages treated with normoxic exosomes. In addition, the phosphorylation level of AKT and mTOR in macrophages treated with hypoxic exosomes derived from pancreatic cancer cells (BxPC-3 and PANC-1) was increased (Fig. 5F and G). To confirm that hypoxic tumor-derived exosomes activate PI3Kγ pathway to promote polarization of macrophages via miR-301a-3p, we transfected miR-301a-3p mimics or inhibitors into macrophages to examine the activation of PTEN/PI3Kγ pathway. As shown in Fig. 5H and I, overexpression of miR-301a-3p in macrophages significantly inhibited the expression of PTEN and promoted the expression of PI3Kγ, p-AKT, and p-mTOR, while inhibition of miR-301a-3p exhibited the opposite effects. To investigate whether exosomal miR-301a-3p regulates macrophages polarization via the PI3Kγ signaling pathway, we further detected the expression of CD206, PI3Kγ, phosphorylation of AKT and mTOR in macrophages treated with PANC-1-H-exo or transfected with miR-301a-3p/mimics posttransfection with PI3Kγ siRNA. As shown in Fig. 5J and K, the expression of CD206, p-AKT, and p-mTOR was downregulated in PI3Kγ knocked down groups. Moreover, both the migration and invasion abilities of PANC-1 cells cocultured with macrophages transfected with PI3Kγ siRNA were decreased regardless of macrophages treated with hypoxic exosomes from PANC-1 cells or transfected with miR-301a-3p/mimics (Fig. 5L–O). PTEN is a negative regulator of PI3K pathway and has been shown to modulate macrophages' polarization (28). Figure 5F–I showed the expression of PTEN was inhibited in macrophages when treated with hypoxic tumor-derived exosomes or transfected with miR-301a-3p/mimics; however, the expression of PTEN was upregulated in macrophages when transfected with miR-301a-3p/inhibitors. Together, these *in vitro* data indicate that hypoxic exosomal miR-301a-3p activates PI3Kγ signaling pathway to induce macrophages polarization via downregulating PTEN expression in macrophages.

Exosomal miR-301a-3p facilitates the lung metastasis of pancreatic cancer cells via inducing M2 macrophage *in vivo*

To further assess the function of exosomal miR-301a-3p in transforming M1–M2 phenotype of macrophages, which stimulate the progression of pancreatic cancer *in vivo*, PANC-1 cells mixed with the conditioned macrophages stimulated by hypoxic PANC-1-exo or transfected by miR-301a-3p/mimics were injected into the mice via tail vein. After 6 weeks, we observed that PANC-1 cells mixed with macrophages treated with PANC-1-H-exo generated more and larger nodules of metastatic lung tumors than those generated by PANC-1 cells alone or mixed with macrophages treated with PANC-1-N-exo group. Likewise, there were significantly more visible and larger lung metastatic nodules in PANC-1+ M-miR-301a-3p/mimics group compared with control group (Fig. 6A and B). Moreover, the weight of mice in the PANC-1+M+H-exo or PANC-1+M-miR-301a-3p/mimics group was significantly lower than that in the control group (Fig. 6C). These results indicate that exosomal miR-301a-3p facilitates pancreatic cancer lung metastasis *in vivo*.

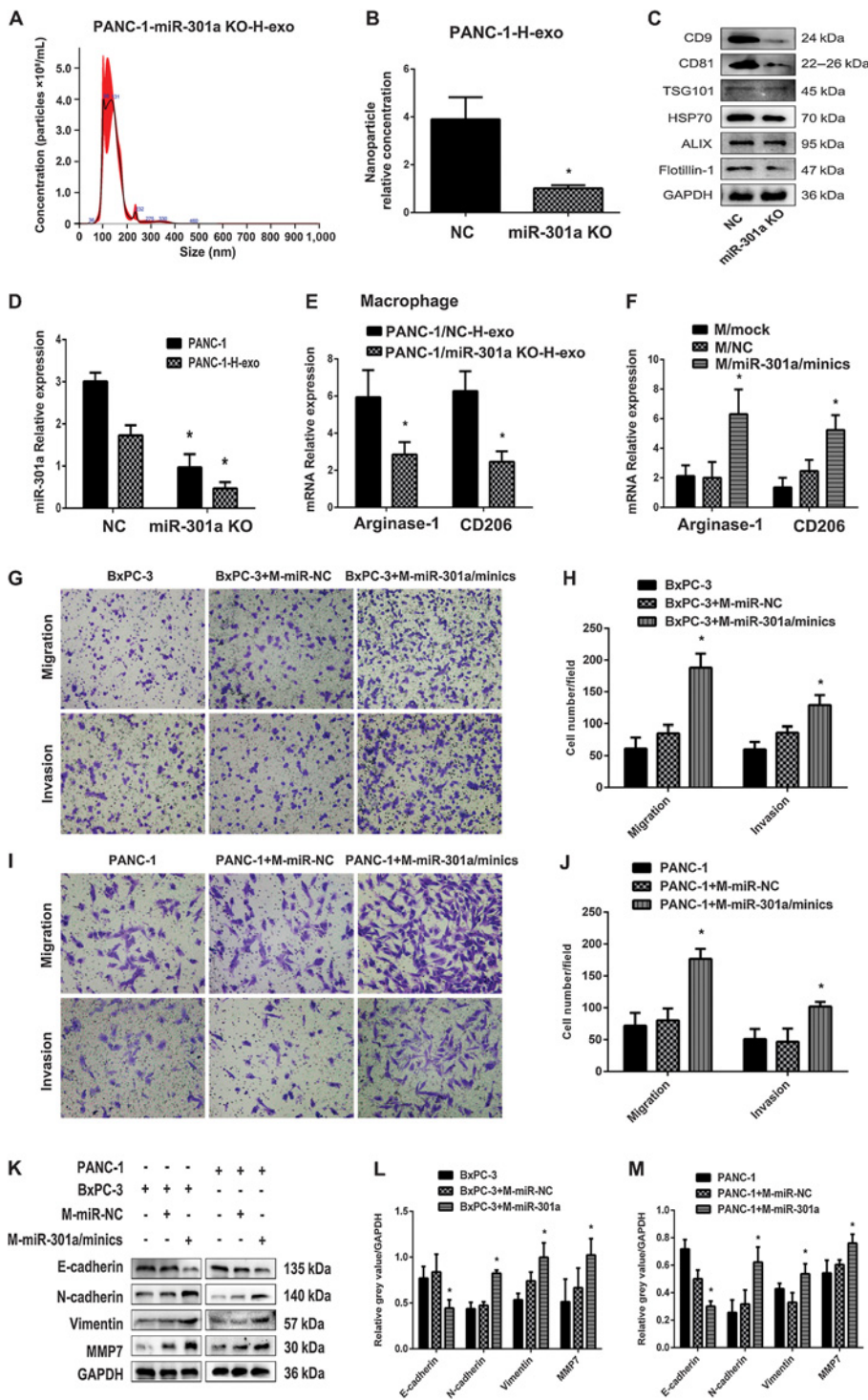


Figure 4. Exosomal miR-301a-3p induces the polarization of M2 macrophages to promote the migration, invasion, and EMT of pancreatic cancer cells. **A–C**, Identical concentrations of miR-301a-3p knockout PANC-1 cells and negative control were seeded under hypoxia. Exosomes (PANC-1-H-exo and PANC-1-miR-301a KO-H-exo) were purified for NTA and Western blot analysis. **A**, NTA analysis of PANC-1-miR-301a KO-H-exo isolated by ultracentrifugation. **B**, PANC-1-exosomes nanoparticles' relative concentration. **C**, Western blot analysis for exosomal proteins CD9, CD81, TSG101, HSP70, ALIX, and Flotillin-1. GAPDH in cell extracts was used as control for cell density. **D**, miR-301a-3p level was analyzed by qRT-PCR in PANC-1 cells and PANC-1-H-exo. **E**, qRT-PCR for CD206 and arginase-1 in macrophages treated for 48 hours with exosomes from miR-301a knockout PANC-1 cells. **F**, qRT-PCR for CD206 and arginase-1 in macrophages transfected with miR-301a-3p/minics (GenePharma). **G** and **I**, Migration and invasion capacity of pancreatic cancer cells (BxPC-3 and PANC-1) cocultured with macrophages transfected with miR-301a-3p/minics was determined using the *in vitro* transwell coculture system. Representative photographs of migratory or invaded cells on the membrane coated with or without Matrigel (magnification, $\times 100$) are shown. **H** and **J**, Morphometric analysis of migratory cells and invaded cells. **K–M**, The effect of the supernatants of macrophages transfected with miR-301a-3p/minics on the EMT of pancreatic cancer cells (BxPC-3 and PANC-1) was analyzed by Western blot analysis. Densitometry shows relative protein expression normalized for GAPDH. Data are shown as mean \pm SD of three independent experiments (*, $P < 0.05$).

Downloaded from <http://aacrjournals.org/cancerres/article-pdf/78/16/4586/2771865/4586.pdf> by guest on 27 August 2022

Discussion

Hypoxia is an important hallmark of solid tumors, and is associated with tumor angiogenesis, glycolysis, growth factor signaling, aggressive phenotypes, and poor prognosis (8, 29). Recently, the involvement of tumor in the malignant evolution of cancers through the release of exosomes has been established, and hypoxia has been postulated to promote exosomes

release from cancer cells (12–15, 30). Exosomes are lipid bilayer-enclosed extracellular vesicles that contain proteins and nucleic acids, especially miRNA. In this study, we purified exosomes from the supernatant of hypoxic pancreatic cancer cells explored the role and underlying mechanisms of exosomal miR-301a-3p in the progression of pancreatic cancer. We found that hypoxia promoted the release of exosomes from

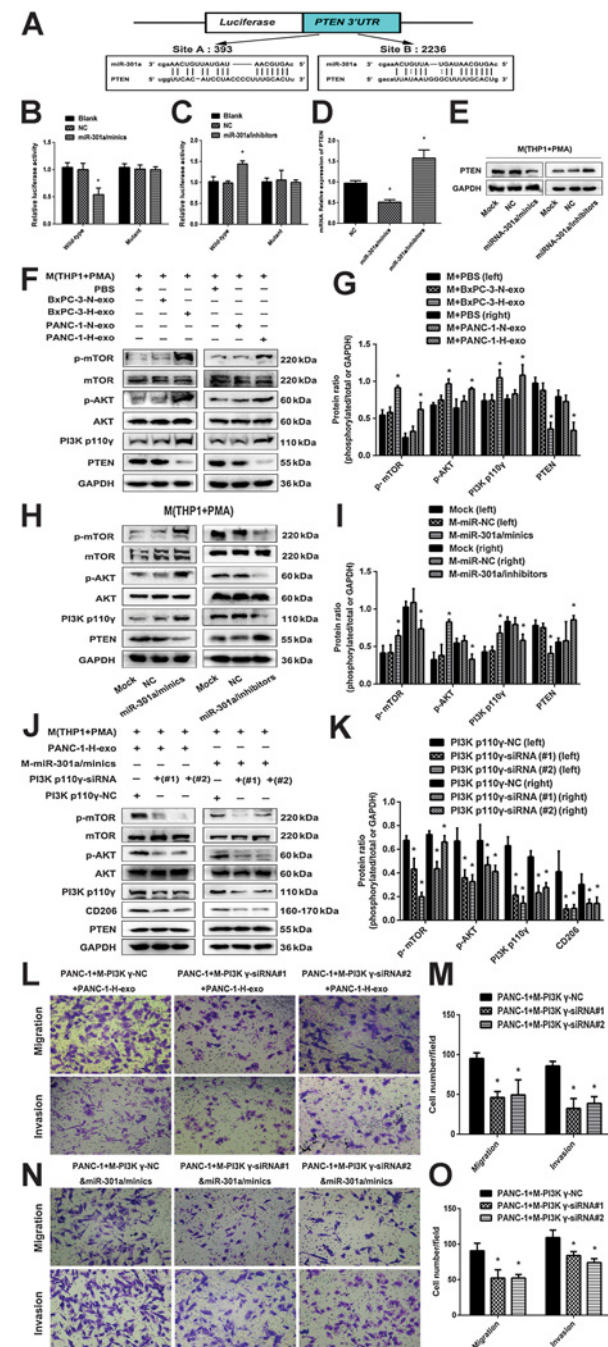


Figure 5. Exosomal miR-301a-3p polarized the M2 macrophage via downregulating PTEN expression and activating PI3K γ signaling pathway. **A**, microRNA.org-Targets and Expression software predicted the miR-301a-3p-binding site in PTEN 3'UTR region. **B** and **C**, Luciferase reporter assays in 293T cells with cotransfection of wild-type or mutant PTEN 3'UTR as well as either miR-301a-3p/mimics or miR-301a-3p/inhibitors (GenePharma) were performed. Luciferase activity was normalized by the ratio of firefly and *Renilla* luciferase signals and determined 48 hours after transfection. **D**, PTEN mRNA was detected by qRT-PCR in 293T cells transfected with miR-301a-3p/mimics or miR-301a-3p/inhibitors. **E**, PTEN protein in macrophages was examined by Western blot posttransfection with miR-301a-3p/mimics or miR-301a-3p/inhibitors. **F**, THP1 treated with PMA

pancreatic cancer cells into circulating system, and the over-expression of serum-derived exosomal miR-301a-3p predicted late TNM stage and poor survival of patients with pancreatic cancer, which suggests that exosomal miR-301a-3p may function as an oncogene in pancreatic cancer and be considered as a marker of cancer occurrence.

Exosomes are secreted by multiple cells, especially tumor cells, and circulate in the blood of patients with cancer, which may be linked to tumor progression (31–33). Recently, accumulated evidences indicate that through communication between tumor cells and surrounding stromal cells, exosomes can create an immune suppression environment promoting tumor progression. Tumor-derived exosomes downregulated expression of NKG2D and repressed NK-cell activity (16, 34). Wieckowski also showed exosomes derived from tumor-promoted T regulatory cell expansion and the demise of antitumor CD8⁺ effector T cells (35). Macrophages, especially M2 macrophages, play dramatic significant roles in tumor initiation and progression, as they can stimulate immune suppression, metastasis, and resistance to anticancer therapy (20, 36, 37). In this study, we found that these hypoxic exosomes induced the alternative activation of macrophage toward M2 phenotype, which promoted the migration, invasion, and EMT of pancreatic cancer cells both *ex vivo* and *in vivo*. Our results suggest that hypoxic exosomes are important components of the tumor microenvironment and act as an important messenger that mediated the cross-talk between cells.

miRNAs are small noncoding RNAs with approximately 22 nucleotides, which can regulate gene expression by binding to the 3' untranslated region (UTR) of specific target mRNAs to inhibit translation or induce degradation. The expression of miRNAs is strictly controlled, and expression dysregulation of miRNAs is linked to cancer (38). miR-301a-3p is a multifunctional miRNA that possesses crucial functions in cancer growth, metastasis, immunity, and inflammation (39–41). Here we demonstrated that miR-301a-3p was significantly rich in exosomes and could be transferred between pancreatic cancer cells and macrophages through exosomes secreted from tumor cells. Hypoxia enhanced miR-301a-3p level in both pancreatic cancer cells and pancreatic cancer cell-derived exosomes, which was

(100 ng/mL; macrophages) for 24 hours was coincubated with hypoxic (or normoxic) exosomes derived from BxPC-3 (or PANC-1) cells. The expression of PTEN and PI3K γ and phosphorylation of AKT and mTOR in macrophages were assessed by Western blot analysis. GAPDH was used as a loading control. **G**, Protein ratio of PTEN, PI3K γ , p-AKT, and p-mTOR in macrophages (*, $P < 0.05$). **H**, The expression of PI3K γ and phosphorylation of AKT and mTOR in macrophages transfected with miR-301a-3p/mimics or miR-301a-3p/inhibitors were examined by Western blot analysis. **I**, Protein ratio of PTEN, PI3K γ , p-AKT, and p-mTOR in macrophages (*, $P < 0.05$). **J**, The expression of CD206 and PI3K γ and phosphorylation of AKT and mTOR in macrophages treated with PANC-1-H-exo or transfected with miR-301a-3p/mimics were examined by Western blot analysis posttransfection with PI3K γ siRNA. **K**, Protein ratio of CD206, PI3K γ , p-AKT, and p-mTOR in macrophages (*, $P < 0.05$). **L** and **M**, The effect of macrophages treated with PANC-1-H-exo and transfected with PI3K γ siRNA on pancreatic cancer cells migration and invasion was determined by the transwell assay. Representative photographs (magnification, $\times 100$) and numbers of migratory or invaded cells are displayed. **N** and **O**, The effect of macrophages cotransfected with miR-301a-3p/mimics and PI3K γ siRNA on pancreatic cancer cell migration and invasion was determined using the transwell assay. Representative photographs (magnification, $\times 100$) and numbers of migratory or invaded cells are displayed. Data are shown as mean \pm SD of three independent experiments (*, $P < 0.05$).

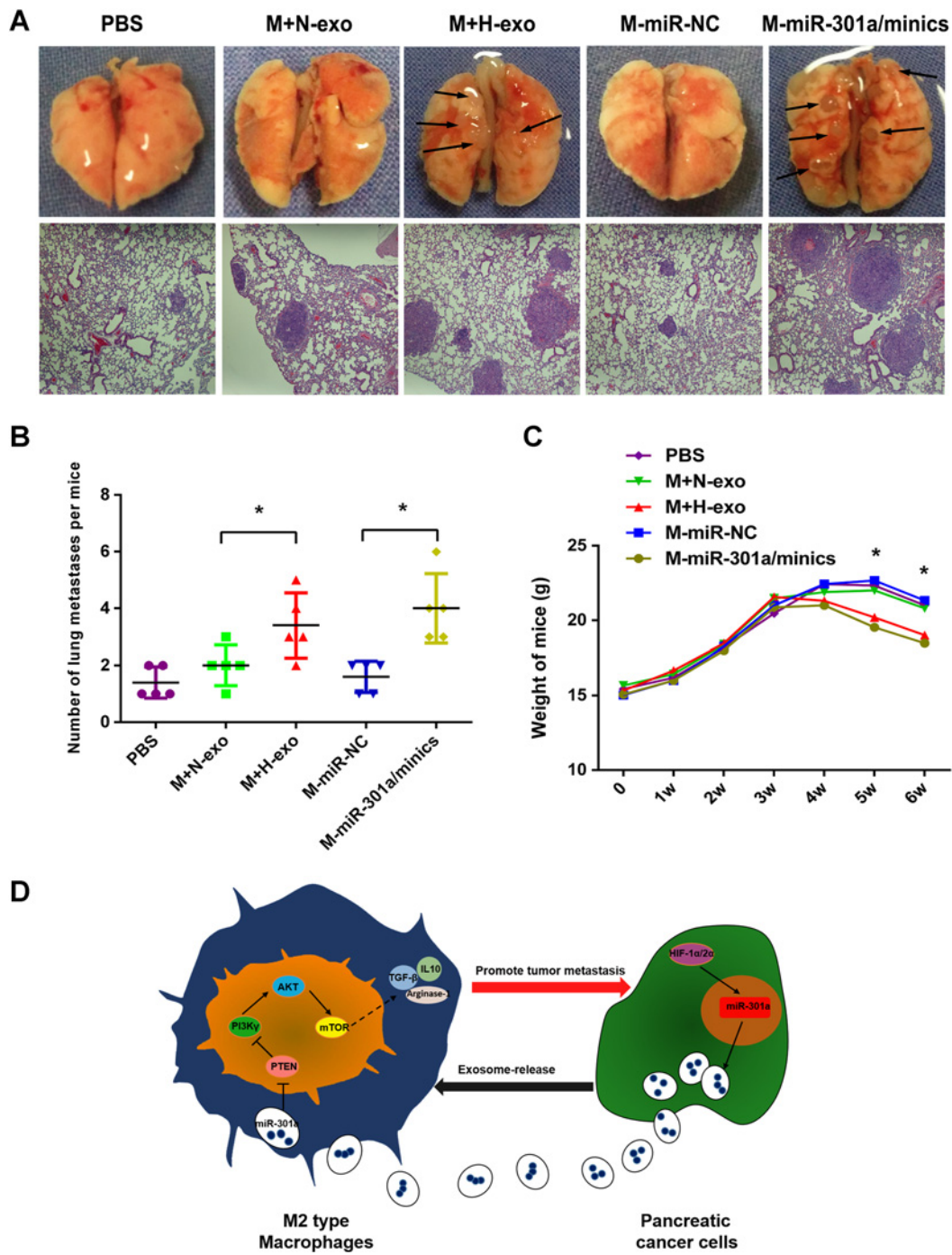


Figure 6. Exosomal miR-301a-3p facilitates the lung metastasis of pancreatic cancer cells via inducing M2 macrophage *in vivo*. **A**, Representative images of lung metastasis in nude mice that resulted from PANC-1 cells alone or PANC-1 cells coinjected with macrophages treated with hypoxic exosomes derived from tumor cells (or transfected with miR-301a-3p/mimics). **B**, The number of metastatic nodules in each indicated group. Data are presented as the mean \pm SD. *, $P < 0.05$. **C**, Weight of nude mice was monitored weekly after being injected with macrophages and PANC-1 cells into the tail veins. **D**, Schematic model of hypoxic exosomal miR-301a-3p promoting macrophages polarization and pancreatic cancer metastasis. Pancreatic cancer cell-derived exosomal miR-301a-3p under hypoxia mediates macrophages M2 polarization via PTEN/PI3K γ signaling pathway, which facilitates the EMT, migration, invasion, and metastatic potential of pancreatic cancer cells.

regulated by HIF-1 α and HIF-2 α . The knockdown of miR-301a-3p in exosomes impaired the exosomes secretion and M2 polarization of macrophages, which was followed by the

decreased migration, invasion, and EMT of pancreatic cancer cells both *ex vivo* and *in vivo*. These results suggest that pancreatic cancer cell-derived exosomal miR-301a-3p plays a crucial

role in the tumor microenvironment interactions and is important for tumor growth and spread.

PI3K p110 γ , belonging to Class I PI3K lipid kinases family, participates partly in the infiltration of myeloid cells into tumors and regulates tumor growth and development via promoting polarization of neutrophils, controlling immune suppression and mediating integrin activation (27, 42–44). Recently, PI3K γ drives transcriptional programming of M2 phenotype macrophages to suppress immune responses and promotes pancreatic ductal adenocarcinoma cell invasion (26). In our study, we showed that activation of PI3K γ signaling by hypoxic exosomal miR-301a-3p promoted differentiation and polarization of M2 macrophages, leading to pancreatic cancer cell migration, invasion, and EMT *in vitro*, as well as lung metastasis *in vivo*. Polarized M2 macrophages promoted transcription of genes associated with the immunosuppressive macrophage phenotype in pancreatic cancer, including immunosuppressive factors such as Arg1, TGF β , and IL10 and chemokines, which may contribute to tumor progression. PTEN loss was inversely correlated with constitutive activation of the PI3K/AKT signaling pathway (28), indicating PTEN inhibits the activation of the PI3K/AKT pathway. PI3K/AKT/mTOR signaling pathway was closely related to macrophage activation and polarization (27, 45). In this study, our results indicate pancreatic cancer-derived exosomes inhibited the expression of PTEN in macrophages and then activated the PI3K γ pathway. miRNAs can bind the 3' UTR location of genes, which inhibit gene expression and then degrade the mRNA. Our previous study has demonstrated that miR-301a confers resistance to gemcitabine by regulating the expression of PTEN (46). In addition, miR-301a promotes tumor growth, migration, and invasion via binding to PTEN in malignant melanoma and breast cancer (47, 48). Our data also show miR-301a-3p targeted the 3' UTR of the *PTEN* gene and inhibited its expression. Then, the decreased expression of PTEN, modulated by miR-301a-3p, resulted in activation of the PI3K/AKT signaling pathway and increasing expression of PI3K γ , p-AKT and p-mTOR. Accordingly, these data reveal miR-301a-3p plays an important role in promoting M2 macrophage polarization by regulating the PTEN/PI3K γ /AKT pathway. Therefore, pancreatic cancer cells can induce the polarization of macrophages toward

M2 phenotypes via miR-301a-3p from pancreatic cancer-derived exosomes.

In summary, we have demonstrated that exosomal miR-301a-3p overexpression predicted late TNM stage and poor survival in human pancreatic cancer, and that hypoxic pancreatic cancer cell-derived exosomal miR-301a-3p induced macrophages M2 polarization by activation of the PTEN/PI3K γ pathway, which promoted pancreatic cancer cells' migration, invasion, and EMT (Fig. 6D). These findings shed light on the mechanism of exosomal miR-301a-3p in the progression of human pancreatic cancer and highlight this pathway as a diagnostic and therapeutic target in the treatment of pancreatic cancer.

Disclosure of Potential Conflicts of Interest

No potential conflicts of interest were disclosed.

Authors' Contributions

Conception and design: L. Su, Z. Qiu

Development of methodology: X. Wang, G. Luo, K. Zhang

Acquisition of data (provided animals, acquired and managed patients, provided facilities, etc.): X. Wang, G. Luo, J. Cao, C. Huang, T. Jiang

Analysis and interpretation of data (e.g., statistical analysis, biostatistics, computational analysis): X. Wang

Writing, review, and/or revision of the manuscript: X. Wang, C. Huang

Administrative, technical, or material support (i.e., reporting or organizing data, constructing databases): C. Huang

Study supervision: B. Liu

Acknowledgments

This work was supported by the National Natural Science Foundation of China (no. 81372640 to Z. Qiu; no. 81572798 to L. Su), Doctoral Innovation Fund Projects from Shanghai Jiao Tong University School of Medicine (no. BXJ201836 to X. Wang), Shanghai Municipal Education Commission-Gaofeng Clinical Medicine Grant Support (no. 20152505 to L. Su), and Shanghai Sailing Program (no. 17YF1415700 to X. Xia).

The costs of publication of this article were defrayed in part by the payment of page charges. This article must therefore be hereby marked *advertisement* in accordance with 18 U.S.C. Section 1734 solely to indicate this fact.

Received December 12, 2017; revised April 18, 2018; accepted June 4, 2018; published first June 7, 2018.

References

1. Bijlsma MF, van Laarhoven HW. The conflicting roles of tumor stroma in pancreatic cancer and their contribution to the failure of clinical trials: a systematic review and critical appraisal. *Cancer Metastasis Rev* 2015;34:97–114.
2. Ryan DP, Hong TS, Bardeesy N. Pancreatic adenocarcinoma. *N Engl J Med* 2014;371:2140–1.
3. Quaresma M, Coleman MP, Rachet B. 40-year trends in an index of survival for all cancers combined and survival adjusted for age and sex for each cancer in England and Wales, 1971–2011: a population-based study. *Lancet* 2015;385:1206–18.
4. Stathis A, Moore MJ. Advanced pancreatic carcinoma: current treatment and future challenges. *Nat Rev Clin Oncol* 2010;7:163–72.
5. Su D, Yamaguchi K, Tanaka M. The characteristics of disseminated tumor cells in pancreatic cancer: a black box needs to be explored. *Pancreatol* 2005;5:316–24.
6. Ackerman D, Simon MC. Hypoxia, lipids, and cancer: surviving the harsh tumor microenvironment. *Trends Cell Biol* 2014;24:472–8.
7. Lewis CE, Pollard JW. Distinct role of macrophages in different tumor microenvironments. *Cancer Res* 2006;66:605–12.
8. Lu X, Kang Y. Hypoxia and hypoxia-inducible factors: master regulators of metastasis. *Clin Cancer Res* 2010;16:5928–35.
9. Lofstedt T, Fredlund E, Holmquist-Mengelbier L, Pietras A, Ovenberger M, Poellinger L, et al. Hypoxia inducible factor-2 α in cancer. *Cell Cycle* 2007;6:919–26.
10. Semenza GL. Defining the role of hypoxia-inducible factor 1 in cancer biology and therapeutics. *Oncogene* 2010;29:625–34.
11. Wahlgren J, De LKT, Brissler M, Vaziri Sani F, Telemo E, Sunnerhagen P, et al. Plasma exosomes can deliver exogenous short interfering RNA to monocytes and lymphocytes. *Nucleic Acids Res* 2012;40:e130.
12. Skog J, Wurdinger T, van Rijn S, Meijer DH, Gainche L, Sena-Esteves M, et al. Glioblastoma microvesicles transport RNA and proteins that promote tumour growth and provide diagnostic biomarkers. *Nat Cell Biol* 2008;10:1470–6.
13. King HW, Michael MZ, Gleadle JM. Hypoxic enhancement of exosome release by breast cancer cells. *BMC Cancer* 2012;12:421.
14. Qu JL, Qu XJ, Zhao MF, Teng YE, Zhang Y, Hou KZ, et al. Gastric cancer exosomes promote tumour cell proliferation through PI3K/Akt and MAPK/ERK activation. *Dig Liver Dis* 2009;41:875–80.

15. Hood JL, San RS, Wickline SA. Exosomes released by melanoma cells prepare sentinel lymph nodes for tumor metastasis. *Cancer Res* 2011; 71:3792–801.
16. Mincheva-Nilsson L, Baranov V. Cancer exosomes and NKG2D receptor-ligand interactions: impairing NKG2D-mediated cytotoxicity and anti-tumor immune surveillance. *Semin Cancer Biol* 2014;28:24–30.
17. Li L, Li C, Wang S, Wang Z, Jiang J, Wang W, et al. Exosomes derived from hypoxic oral squamous cell carcinoma cells deliver miR-21 to normoxic cells to elicit a prometastatic phenotype. *Cancer Res* 2016;76:1770–80.
18. Gordon S, Martinez FO. Alternative activation of macrophages: mechanism and functions. *Immunity* 2010;32:593–604.
19. Singh A, Talekar M, Raikar A, Amiji M. Macrophage-targeted delivery systems for nucleic acid therapy of inflammatory diseases. *J Control Release* 2014;190:515–30.
20. Wang J, Cao Z, Zhang XM, Nakamura M, Sun M, Hartman J, et al. Novel mechanism of macrophage-mediated metastasis revealed in a zebrafish model of tumor development. *Cancer Res* 2015;75:306–15.
21. Yin M, Li X, Tan S, Zhou HJ, Ji W, Bellone S, et al. Tumor-associated macrophages drive spheroid formation during early transcoelomic metastasis of ovarian cancer. *J Clin Invest* 2016;126:4157–73.
22. Thery C, Amigorena S, Raposo G, Clayton A. Isolation and characterization of exosomes from cell culture supernatants and biological fluids. *Curr Protoc Cell Biol* 2006;3:Unit 3 22.
23. Kroh EM, Parkin RK, Mitchell PS, Tewari M. Analysis of circulating microRNA biomarkers in plasma and serum using quantitative reverse transcription-PCR (qRT-PCR). *Methods* 2010;50:298–301.
24. Mathivanan S, Fahner CJ, Reid GE, Simpson RJ. ExoCarta 2012: database of exosomal proteins, RNA and lipids. *Nucleic Acids Res* 2012;40:D1241–4.
25. Liao J, Liu R, Yin L, Pu Y. Expression profiling of exosomal miRNAs derived from human esophageal cancer cells by Solexa high-throughput sequencing. *Int J Mol Sci* 2014;15:15530–51.
26. Kaneda MM, Cappello P, Nguyen AV, Ralainirina N, Hardamon CR, Foubert P, et al. Macrophage PI3Kgamma drives pancreatic ductal adenocarcinoma progression. *Cancer Discov* 2016;6:870–85.
27. Kaneda MM, Messer KS, Ralainirina N, Li H, Leem CJ, Gorjestani S, et al. PI3Kgamma is a molecular switch that controls immune suppression. *Nature* 2016;539:437–42.
28. Pfeifer M, Grau M, Lenze D, Wenzel SS, Wolf A, Wollert-Wulf B, et al. PTEN loss defines a PI3K/AKT pathway-dependent germinal center subtype of diffuse large B-cell lymphoma. *Proc Natl Acad Sci U S A* 2013;110:12420–5.
29. Vaupel P, Mayer A. Hypoxia in cancer: significance and impact on clinical outcome. *Cancer Metastasis Rev* 2007;26:225–39.
30. Clayton A, Mitchell JP, Court J, Linnane S, Mason MD, Tabi Z. Human tumor-derived exosomes down-modulate NKG2D expression. *J Immunol* 2008;180:7249–58.
31. Melo SA, Luecke LB, Kahlert C, Fernandez AF, Gammon ST, Kaye J, et al. Glypican-1 identifies cancer exosomes and detects early pancreatic cancer. *Nature* 2015;523:177–82.
32. Allenson K, Castillo J, San Lucas FA, Scelo G, Kim DU, Bernard V, et al. High prevalence of mutant KRAS in circulating exosome-derived DNA from early-stage pancreatic cancer patients. *Ann Oncol* 2017;28:741–7.
33. Madhavan B, Yue S, Galli U, Rana S, Gross W, Muller M, et al. Combined evaluation of a panel of protein and miRNA serum-exosome biomarkers for pancreatic cancer diagnosis increases sensitivity and specificity. *Int J Cancer* 2015;136:2616–27.
34. Liu C, Yu S, Zinn K, Wang J, Zhang L, Jia Y, et al. Murine mammary carcinoma exosomes promote tumor growth by suppression of NK cell function. *J Immunol* 2006;176:1375–85.
35. Wiecekowi EU, Visus C, Szajnik M, Szczepanski MJ, Storkus WJ, Whiteside TL. Tumor-derived microvesicles promote regulatory T cell expansion and induce apoptosis in tumor-reactive activated CD8+ T lymphocytes. *J Immunol* 2009;183:3720–30.
36. Ruffell B, Coussens LM. Macrophages and therapeutic resistance in cancer. *Cancer Cell* 2015;27:462–72.
37. Zhu Y, Knolhoff BL, Meyer MA, Nywening TM, West BL, Luo J, et al. CSF1/CSF1R blockade reprograms tumor-infiltrating macrophages and improves response to T-cell checkpoint immunotherapy in pancreatic cancer models. *Cancer Res* 2014;74:5057–69.
38. Acunzo M, Romano G, Wernicke D, Croce CM. MicroRNA and cancer—a brief overview. *Adv Biol Regul* 2015;57:1–9.
39. Wang M, Li C, Yu B, Su L, Li J, Ju J, et al. Overexpressed miR-301a promotes cell proliferation and invasion by targeting RUNX3 in gastric cancer. *J Gastroenterol* 2013;48:1023–33.
40. Hazra B, Kumawat KL, Basu A. The host microRNA miR-301a blocks the IRF1-mediated neuronal innate immune response to Japanese encephalitis virus infection. *Sci Signal* 2017;10:eaaf5185.
41. He C, Shi Y, Wu R, Sun M, Fang L, Wu W, et al. miR-301a promotes intestinal mucosal inflammation through induction of IL-17A and TNF-alpha in IBD. *Gut* 2016;65:1938–50.
42. Li Z, Jiang H, Xie W, Zhang Z, Smrcka AV, Wu D. Roles of PLC-beta2 and -beta3 and PI3Kgamma in chemoattractant-mediated signal transduction. *Science* 2000;287:1046–9.
43. Schmid MC, Franco I, Kang SW, Hirsch E, Quilliam LA, Varner JA. PI3-kinase gamma promotes Rap1a-mediated activation of myeloid cell integrin alpha4beta1, leading to tumor inflammation and growth. *PLoS One* 2013;8:e60226.
44. Schmid MC, Avraamides CJ, Dippold HC, Franco I, Foubert P, Ellies LG, et al. Receptor tyrosine kinases and TLR/IL1Rs unexpectedly activate myeloid cell PI3Kgamma, a single convergent point promoting tumor inflammation and progression. *Cancer Cell* 2011;19:715–27.
45. Rocher C, Singla DK. SMAD-PI3K-Akt-mTOR pathway mediates BMP-7 polarization of monocytes into M2 macrophages. *PLoS One* 2013;8:e84009.
46. Xia X, Zhang K, Luo G, Cen G, Cao J, Huang K, et al. Downregulation of miR-301a-3p sensitizes pancreatic cancer cells to gemcitabine treatment via PTEN. *Am J Transl Res* 2017;9:1886–95.
47. Cui L, Li Y, Lv X, Li J, Wang X, Lei Z, et al. Expression of MicroRNA-301a and its functional roles in malignant melanoma. *Cell Physiol Biochem* 2016;40:230–44.
48. Shi W, Gerster K, Alajez NM, Tsang J, Waldron L, Pintilie M, et al. MicroRNA-301 mediates proliferation and invasion in human breast cancer. *Cancer Res* 2011;71:2926–37.